Published in final edited form as:

IEEE Trans Appl Supercond. 2012 June ; 22(3): . doi:10.1109/TASC.2011.2178976.

No-Insulation (NI) HTS Inserts for > 1 GHz LTS/HTS NMR Magnets

Seungyong Hahn, **Dong Keun Park**, **John Voccio**, **Juan Bascuñán**, and **Yukikazu Iwasa**

Francis Bitter Magnet Laboratory, Massachusetts Institute of Technology, Cambridge, MA 02139 USA

Abstract

A no-insulation (NI) technique has been applied to wind and test a NI HTS (YBCO) double-pancake coil at 4.2 K. Having little detrimental effect on field-current relationship, the absence of turn-to-turn insulation enabled the test coil to survive a quench at a coil current density of 1.58 kA/mm^2. The NI HTS coil is compact and self-protecting, two features suitable for large high-field magnets. To investigate beneficial impacts of the NI technique on >1 GHz LTS/HTS NMR magnets, we have designed six new NI HTS inserts for our ongoing 1.3 GHz LTS/HTS NMR magnet, which require less costly LTS background magnets than the original insulated HTS insert. A net result will be a significant reduction in the overall cost of an LTS/HTS NMR magnet, at 1.3 GHz and above.

Keywords

Compact HTS insert magnet; GHz-class NMR; LTS/HTS NMR; no-insulation winding; self-protecting

I. Introduction

FOR an LTS/HTS NMR magnet, the HTS insert must bear the entire share of any incremental frequency increase beyond 1 GHz (23.5 T), because the LTS's share is limited to ≤1 GHz. Thus, for a > 1 GHz LTS/HTS NMR magnet, we must make its HTS insert *high-performance* : specifically its frequency high and o.d. compact, because the two parameters directly impact the cost of the LTS background magnet, the largest cost driver of an > 1 GHz LTS/HTS NMR magnet.

To make the HTS insert of our 1.3 GHz LTS/HTS NMR magnet [1], [2] high performance, we have been exploring an NI (no insulation) technique [3] of which the key idea is to completely eliminate turn-to-turn insulation, metallic or organic [4]–[6], from its winding. Primary benefits of the HTS NI technique over the insulated counterpart include: 1) mechanically robust winding that reduces strain of a winding under a given magnetic stress; 2) enhancement of overall current density, particularly for YBCO tape whose overall

syhahn@mit.edu.

Color versions of one or more of the figures in this paper are available online at http://ieeexplore.ieee.org.

thickness is nearly the same as that of typical insulators; and 3) reduced risks of over-heating upon a local quench spot. Recently, we reported test results of the first-ever prototype NI HTS pancake coils operated at 77 K, which demonstrated that compact and stable HTS windings are feasible [3].

A new NI HTS coil having a larger inductance has been constructed and tested in a bath of LHe (liquid helium) to investigate its field performance and thermal stability at 4.2 K. On the strength of these encouraging results, we have designed six alternate HTS inserts, all based on the NI technique, for our on-going 1.3 GHz LTS/HTS NMR magnet in particular and to emphasize the beneficial impacts of the NI technique on > 1 GHz LTS/HTS NMR magnets in general. The new HTS inserts cover the frequency range 600–800 MHz with room-temperature (RT) bores of either 54 or 60 mm. This paper presents: 1) test results and analyses of the new NI HTS coil at 4.2 K; and 2) design and stress analyses of the six HTS inserts and comparison with our 600-MHz/54-mm (H600–54) HTS *insulated* insert currently under construction [2]. Potential challenges of the NI technique are also discussed.

II. Test of Single Pancake NI HTS Coil at 4.2 K

A. Construction of NI HTS Test Coil

The test NI HTS coil was wound with YBCO conductor currently used to construct the H600–54. Fig. 1(a) shows a picture of the test NI HTS coil having 210 turns with winding i.d. ($2a_2$) and o.d. ($2a_2$) of 25.4 mm and 53.2 mm, respectively; the α, defined by a_2/a_1, is 2.1 so the coil may be considered as a *thick* pancake. Key parameters of the coil and conductor are summarized in Table I. Note that Cu layer in this conductor is only 5-μm thick per side. Fig. 1(b) shows the test NI HTS coil installed in the LHe test setup. The conductors external to the coil were tripled for protection in over-current tests.

B. Test Results and Discussion

The test coil at 4.2 K was charged at a rate of 0.1 A/s to a target operating current of either 50 A or 125 A, held at a target current for 400 s, and discharged at a rate of 0.1 A/s. Fig. 2 presents the test results: open and solid symbols stand for the respective 50 A and 125 A target currents, while squares, circles, and diamonds respectively for power supply currents (I_p), measured axial field (B_z) at the coil center, and calculated B_z of its insulated (INS) counterpart of which size and number of turns are identical to those of the NI coil. Except for a charging delay of 90 s, barely discernible from Fig. 2, the NI coil fields match well to the calculated INS counterpart fields. The charging delay was previously discussed in detail with an equivalent circuit model of an NI coil [3].

Fig. 3 shows the results of an over-current test for investigating thermal stability of an NI coil at 4.2 K. With the supply current in manual control, the coil *fully* quenched at 486 A (t = 168 s). From the measured center field of 2.87 T, we estimate a field generating current of 412 A (corresponding conductor current density of 1.58 kA/mm^2) that flows through the winding spiral path while the balance of 74 A bypassing through the turn-to-turn contacts. Note that the bypass current is proportional to the current ramping rate according to the equivalent circuit model in [3]. Upon the quench, the power supply current increased slowly

to 492 A when the current lead voltages started rising at t = 188 s. Finally, during the discharge mode, a section external to the coil (white dashed box in Fig. 1(a)) burned out at t = 203 s (397 A) though a subsequent test at 77 K confirmed that the coil itself was undamaged. In a separate 77-K short sample test, the conductor burned out at 90 A, which corresponds to a conductor current density of only 350 A/mm^2.

The results prove that even a *thick* ($\alpha > 2$) NI HTS coil appears to be thermally stabile at a current density as large as 1.58 kA/mm^2 in a bath of LHe at 4.2 K. They also imply that an NI HTS magnet may not require active protection. Equally important, with stabilizer matrix nominally needed for protection but eliminated from the winding, a *self-protecting* NI coil can be compact, i.e., the overall current density is significantly enhanced. Clearly, before the NI technique can be applied to an HTS insert for >1-GHz LTS/HTS NMR magnets, there are other issues to be resolved, both quench-induced: 1) unbalancing axial forces resulting from current misdistribution; and 2) transient internal voltages. Also, the charging delay requires further study.

III. Design of No-Insulation HTS Inserts

Here, we present designs of the 600-MHz/54-mm HTS insert (H600–54) [6] plus of six new NI HTS inserts: 1) H600N −54; 2) H600N-60; 3) H700N-54; 4) H700N-60; 5) H800N-54 and 6) H800N-60. Each insert consists of two nested coils, inner and outer, each a stack of double-pancake (DP) coils wound with YBCO (inner) and Bi2223 (outer) conductors. The six inner YBCO coils are of NI type, while the outer coils are co-wound with reinforcing stainless steel strip.

A. Conductor Design

Table II presents key elastic properties of the windings for H600–54 and six NI options, computed by mixture rule and finite element method applied to winding component properties. In the H600–54 inner coil, a 0.25-mm thick Cu strip was co-wound for protection [7]. As Cu yields, the effective Young's modulus (E) of Cu is 40 GPa [7]. With the Cu strip absent in the new inner coils, their equivalent anisotropic Young's moduli are larger than that of the H600–54 inner coil.

B. Magnet Design

Table III summarizes key parameters of H600-54 and new six NI HTS inserts with a 1 H NMR frequency of 600, 700, or 800 MHz and an RT bore of either 54 or 60 mm. Those inserts with a 60-mm RT bore are designed to accommodate extra shim sets to mitigate large field impurities of screening-cur-rent-induced fields [8], [9]. Design focuses are to: 1) limit the overall hoop strain to less than 0.5% and 0.4% for YBCO and Bi2223 coils respectively, though the maximum tensile strain limits are 0.6% for YBCO and 0.45% for Bi2223 [7]; 2) set a radial gap of 26 mm between the inner coil and the RT bore (20 mm in HT600–54) for improved cryogenics; 3) set an operating current, I_{op}, 180–210 A, less than the 251 A of H600–54. The overall current densities of the new inner coils, 46–54 kA/cm^2, are 2.3–2.7 times larger than that of H600–54. As a result, the new inner coils are more compact and mechanically robust (less strained) than H600–54. Also, each new inner coil, though having

an i.d. larger than that of H600–54 and an o.d. even smaller, contributes a greater center field than H600–54.

As an HTS insert becomes compact, the cold bore of the back-ground LTS magnet become smaller. Included in Table III are the frequencies and cold bore sizes of the respective background LTS magnets for a 1.3 GHz LTS/HTS magnet. Fig. 4 shows to-scale drawings of all the HTS inserts.

C. Stress Analysis and Discussion

The largest stress and strain, at the axial midplane, of each insert, are computed with force equilibrium, (1) and generalized Hook's laws, (2) and (3), with the plane strain assumption, (4). Here, r, σ, ε, E, v, J, B, ε_T, and α_T are, respectively, radius, stress, strain, Young's modulus, Poisson ratio, current density, magnetic field, thermal strain, and thermal expansion coefficient. The bending strains are given by $d/2r$, where d is the distance between the conductor neutral axis and the supercon-ductor layer: 0.05 mm (YBCO) and 0.23 mm (Bi2223).

$$r\frac{\partial \sigma_r}{\partial r} + \sigma_r - \sigma_h + rJB = 0 \quad (1)$$

$$\varepsilon_r = \frac{\sigma_r}{E_r} - \nu_{hr}\frac{\sigma_h}{E_h} - \nu_{zr}\frac{\sigma_z}{E_z} + \varepsilon_{Tr}, \quad (2)$$

$$\varepsilon_{Tr} = \int_{77}^{4.2} \alpha_{Tr}(T)dT$$

$$\varepsilon_h = \frac{\sigma_h}{E_h} - \nu_{rh}\frac{\sigma_r}{E_r} - \nu_{zr}\frac{\sigma_z}{E_z} + \varepsilon_{Th}, \quad (3)$$

$$\varepsilon_{Th} = \int_{77}^{4.2} \alpha_{Th}(T)dT$$

$$\sigma_z = \nu_{rz} E_z \frac{\sigma_r}{E_r} + \nu_{hz} E_z \frac{\sigma_h}{E_h} - E_z \varepsilon_{Tz}, \quad (4)$$

$$\varepsilon_{Tz} = \int_{77}^{4.2} \alpha_{Tz}(T) dT$$

Figs. 5(a) and 5(b) shows calculated overall hoop strains, on the midplane, including magnetic, thermal, and bending, for the respective 54- and 60-mm RT bore inserts. Each insert is assumed to have stainless steel overbanding of a 5-mm build and to be operated with a respective LTS background magnet to generate the 1.3 GHz (30.5 T). The overall hoop strains increase with frequency and size of HTS insert in general. The overall strains of Bi2223 coils are smaller than those of YBCO chiefly owing to the smaller overall current densities (Table III). Note that the strains of both YBCO and Bi2223 are maximum at the innermost turn, decreasing with radius, at the outermost turn, to ~40% of the innermost turn.

IV. Conclusion

We believe that the no-insulation (NI) technique may be most suitable for winding an HTS insert, which must bear an increasingly large share of the total field in a >1 GHz (23.5 T) LTS/HTS NMR magnet. A compact, high-performance, and self-protecting NI HTS insert leads to a less costly LTS magnet. Because the overall cost a > 1 GH_Z LTS/HTS NMR magnet is primarily driven by the cost of the LTS magnet, its reduction is a major benefit of the NI technique. The test results have confirmed that the absence of turn-to-turn insulation in NI HTS double-pancake coils may greatly benefit their protection with little detrimental effects on their field-current relationship. For our ongoing 1.3 GHz LTS/HTS NMR magnet project, six new LTS/HTS magnet options have been designed, which require less costly LTS background magnets than the original insulated insert. The NI technique should contribute to the significant cost reduction of >1 GHz LTS/HTS NMR magnets.

Acknowledgment

The authors thank the NCRR, NIBIB, and NIGMS of the National Institutes of Health for their continued support of our on-going 1.3 GHz LTS/HTS NMR magnet project.

This work was supported by the National Center for Research Resources, National Institute for Biomedical Imaging and Bioengineering, and National Institute of General Medical Sciences, all of the National Institutes of Health.

References

[1]. Iwasa Y, Bascuñán J, Hahn S, Tomita M, and Yao W, “High-temperature superconducting magnets for NMR and MRI: R&D activities at the MIT francis bitter magnet laboratory,” IEEE Trans. Appl. Super-cond, vol. 20, no. 3, pp. 718–721, 2010.

[2]. Bascuñán J, Hahn S, Park DK, and Iwasa Y, “A 1.3-GHz LTS/HTS NMR Magnet—A progress report,” IEEE Trans. Appl. Supercond, vol. 21, no. 3, pp. 2092–2095, 2011. [PubMed: 22081752]

[3]. Hahn S, Park DK, Bascuñán J, and Iwasa Y, “HTS pancake coils without turn-to-turn insulation,” IEEE Trans. Appl. Supercond, vol. 21, no. 3, pp. 1592–1595, 2011.

[4]. Bailey RE, Burgeson J, Magnuson G, and Parmer J, "Metallic Insulation for Superconducting Coils," U.S. Patent 4 760 365, 1988.

[5]. Dudarev AV et al., "Superconducting windings with "short-circuited" turns," Inst. Phys. Conf. ser No 158, pp. 1615–1619, 1998.

[6]. Evans D, "Turn, layer, and ground insulation for superconducting magnets," Physica C, vol. 354, pp. 136–142, 2001.

[7]. Hahn S, Bascuñán J, Yao W, and Iwasa Y, "Two HTS options for a 600 MHz insert of a 1.3 GHz LTS/HTS NMR magnet: YBCO and BSCCO," Physica C, vol. 470, no. 20, pp. 1721–1726, 2010.

[8]. Ahn MC et al., "Spatial and temporal variations of a screening current induced magnetic field in a double-pancake HTS insert of an LTS/HTS NMR magnet," IEEE Trans. Appl. Supercond, vol. 19, pp. 2269–2272, 2009. [PubMed: 20401187]

[9]. Amemiya N and Akachi K, "Magnetic field generated by shielding current in high Tc superconducting coils for NMR magnets," Super-cond. Sci. Technol, vol. 21, p. 095001, 2008

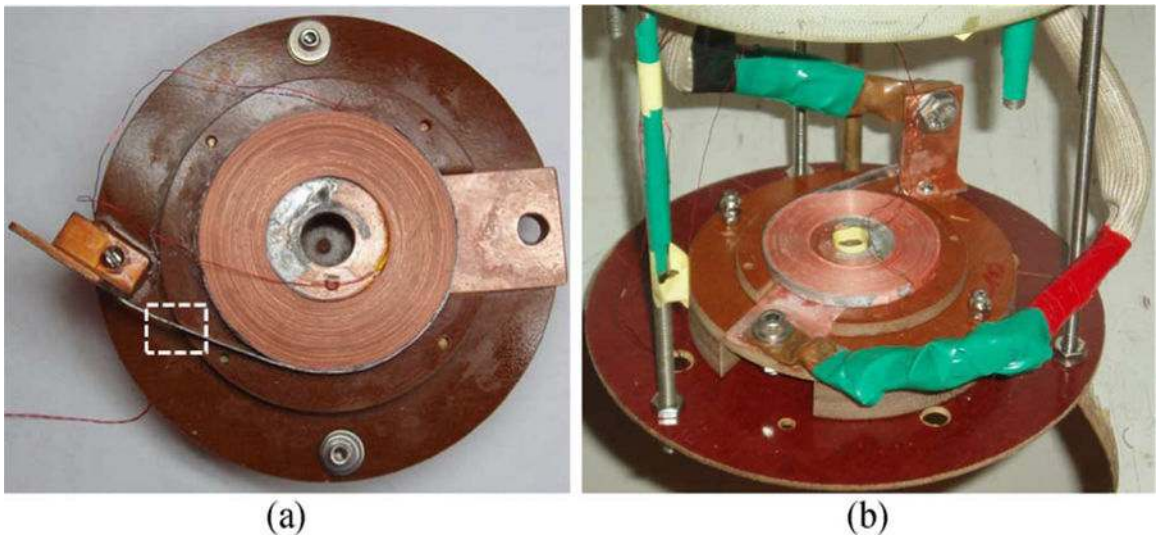

Fig. 1.
(a) NI HTS single pancake test coil; (b) Test coil mounted in the LHe experimental setup.

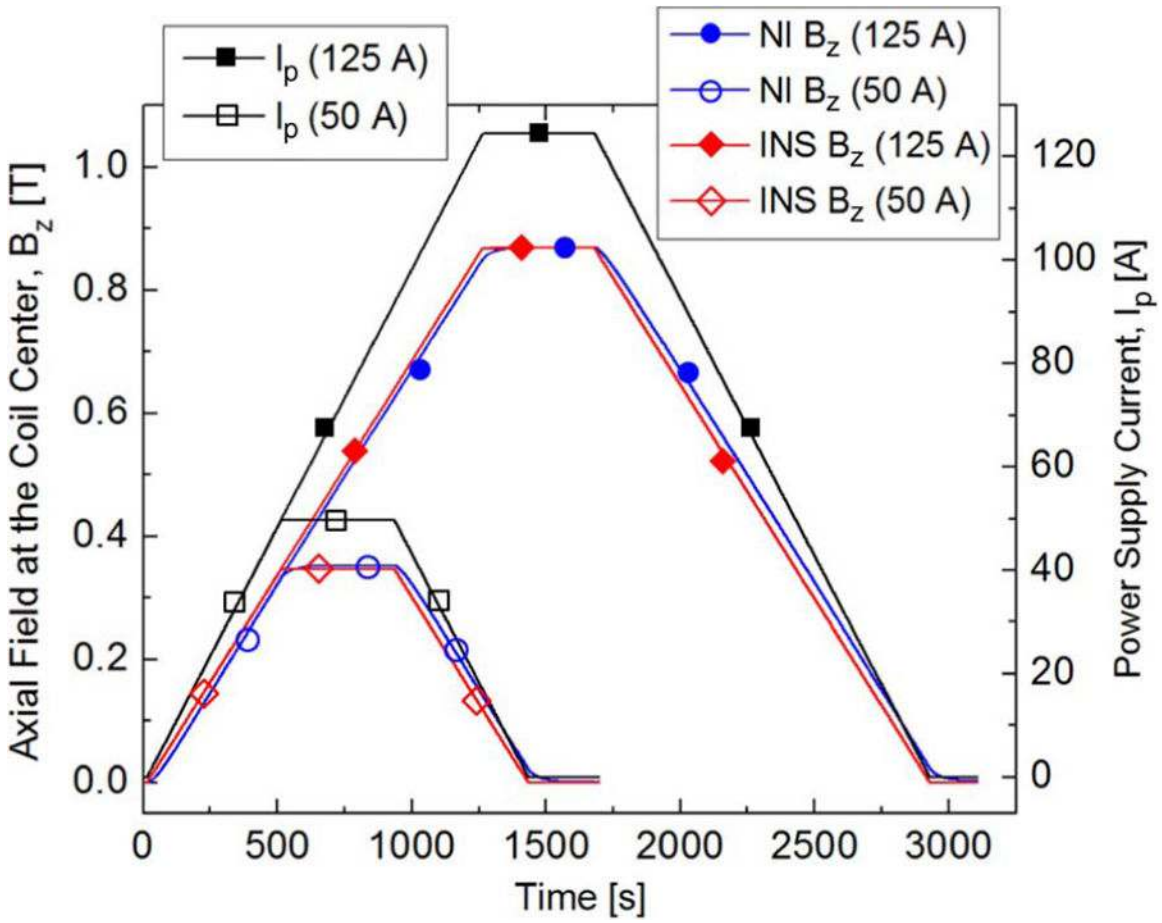

Fig. 2.
Charge-discharge test results of the NI HTS test coil at 4.2 K.

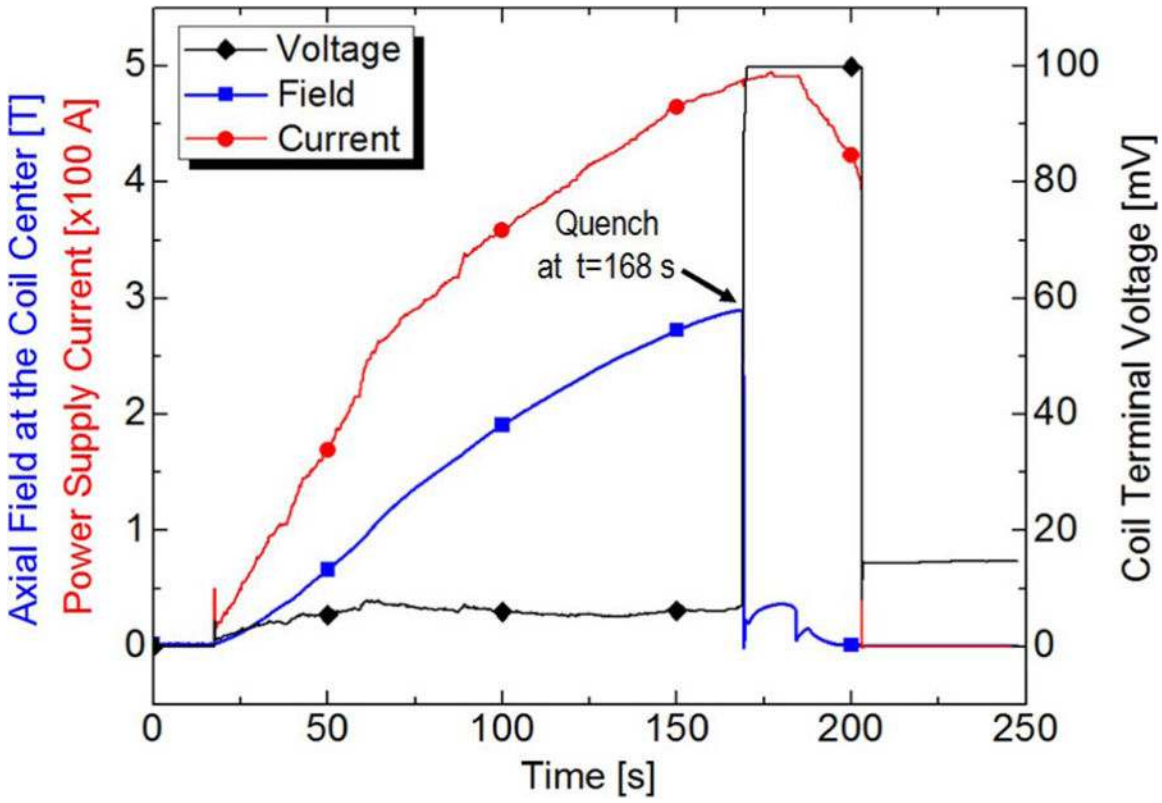

Fig. 3.
Overcurrent test results of the NI HTS test coil at 4.2 K.

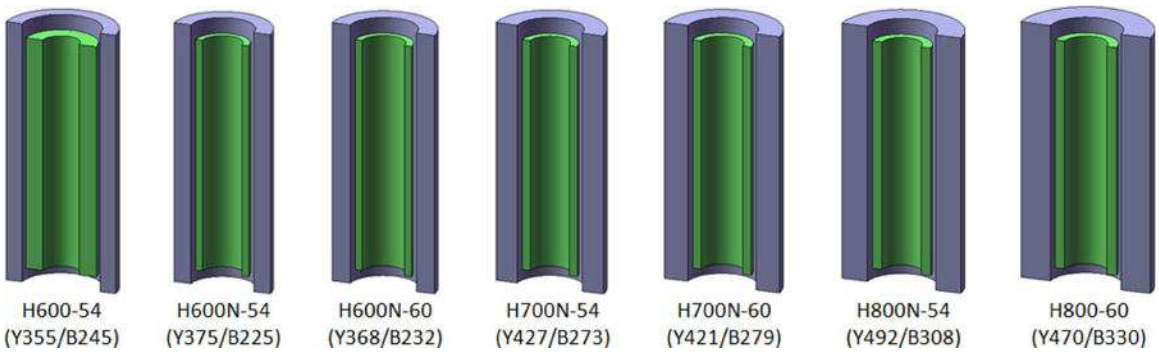

Fig. 4.

To-scale drawings of H600–54 and six new inserts. In the parenthesis are frequency contributions from YBCO (Y)/Bi2223 (B) coils.

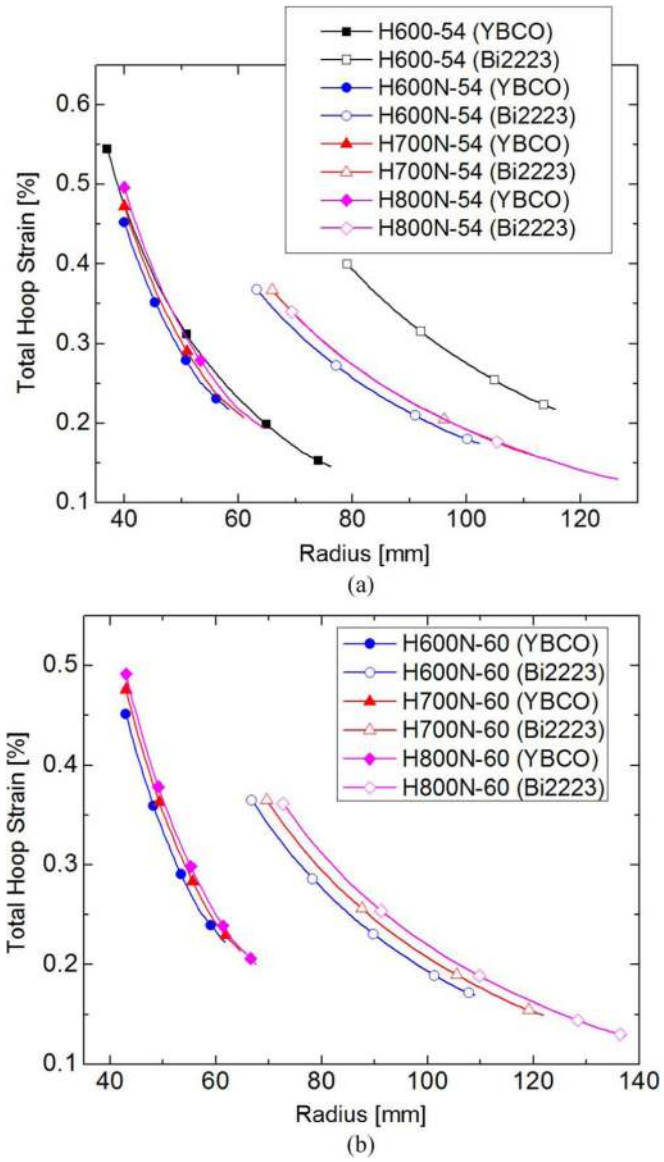

Fig. 5.

Overall computed strains including magnetic, thermal, and bending strains on axial midplane of (a) 54-mm and (b) 60-mm RT bore inserts

TABLE I

KEY PARAMETERS OF YBCO TEST COIL

Parameters		Values
Conductor		
Overall width; thickness	[mm]	4.0; 0.065
Cu stabilizer thickness	[μm]	10(5 per each side)
Critical current @ 77 k. self	[A]	80 – 100
Coil		
i.d. ($2a_1$); o.d ($2a_2$).; height (h)	[mm]	25.4; 53.2; 4.0
Turns; layers		210; 1 (single pancake)
Inductance	[mH]	1.87
Magnet constant (B_z @ 1 A)	[mT]	6.97
Charging time constant	[s]	30
Coil critical current @ 77k, self	[A]	48

TABLE II

ELASTIC PROPERTIES OF HTS WINDINGS BY MIXTURE RULE AND FINITE ELEMENT METHOD [7]

Parameters		**YBCO (H600–54)**		**Bi2223**		**YBCO (NI)**	
Material		Hastelloy	Cu	HT-SS	SS	Hastelloy	Cu
Width	**[mm]**	4.0	4.0	4.5	4.5	4.0	4.0
Thickness	**[mm]**	0.055	0.25 *	0.3	0.05	0.055	0.04
E	**[GPa]**	197	40	68	207	197	40
Equivalent anisotropic properties by mixture rule and FEM							
Er; Eh; Ez	**[GPa]**	46.0; 66.9; 66.5		73.8; 86.0; 84.4		72.7; 128; 121	
ν_{rh}; ν_{hz}; ν_{rz}		0.37; 0.33; 0.23		0.35; 0.34; 0.28		0.39; 0.35; 0.20	
+ ε_{Tr}; ε_{Th}; ε_{Tz}	[%]	0.041; 0.041; 0.044		0.049; 0.049; 0.051		0.041; 0.041; 0.044	

* Including a 0.02-mm adhesive organic insulation

+ Anisotropic thermal expansion between 4 K and 77 K

IEEE Trans Appl Supercond. Author manuscript; available in PMC 2019 May 09.

TABLE III

KEY PARAMETERS OF THE H600–54 and the Newly Designed NI HTS Inserts

	H600–54		H600N-54		H600N-60		H700N-54		H700N-60		H800N-54		H800N-60	
	YBCO	**Bi2223**	**YBCO**	**Bi2223**	**YBCO**	**Bi2223**	**YBCO**	**Bi2223**	**YBCO**	**Bi2223**	**YBCO**	**Bi2223**	**YBCO**	**Bi2223**
Frequency [MHz]	355	245	375	225	368	232	427	273	421	279	492	308	470	330
Field contribution [T]	8.33	5.76	8.80	5.29	8.63	5.46	10.02	6.42	9.89	6.55	11.56	7.22	11.03	7.75
Wire I_c @ 77 K. sf [A]	>110	>160	>110	>160	>100	>150	>100	>150	>100	>140	>100	>140	>100	>130
I_c.($B_\perp$.42K)/I_c(sf.77K)	>3	>2.2	>2.7	>2.3	2.7	>2.3	>2.5	>2.2	>2.5	>2.2	>2.3	>2.1	>2.3	>2.1
Peak $B_\perp$ in coil at I_{op} [T]	3.9	3.5	5.0	3.0	5.0	3.1	5.4	3.4	5.5	3.5	6.0	3.7	5.9	3.8
Operating current. I_{op} [A]	251.0		210.5		199.9		199.9		190.1		190.4		179.6	
Current density (kA/cm^2)	19.94	15.50	53.69	13.00	50.90	12.34	51.03	12.35	48.56	11.74	48.51	11.76	45.85	11.09
Number of DP	56	56	56	56	56	56	56	56	56	56	56	56	56	56
Turn per pancake	112	90	140	97	145	106	168	125	175	135	204	149	207	171
Inner diameter [mm]	74.0	158 3	80	126.6	86	133.6	80	131.9	86	139.2	80	138.8	86	145.3
Outer diameter [mm]	142.3	221.3	106.6	194.5	113.6	207.8	111.9	219.4	119.2	233.7	118.8	243.1	125.3	265.0
Height [mm]	462.2	518.2	462.2	518.2	462.2	518.2	462.2	518.2	462.2	518.2	462.2	518.2	462.2	518.2
SS overhand build [mm]	5.0	5.0	5.0	5.0	5.0	5.0	5.0	5.0	5.0	5.0	5.0	5.0	5.0	5.0
Wire length/DP [m]	77.6	107.4	82	98	91	114	101	138	113	158	127	179	137	220
Total wire length [km]	4.35	6.02	4.6	5.5	5.1	6.4	5.7	7.7	6.3	8.8	7.1	10.0	7.7	12.3
Self inductance [H]	2.88	5.31	3.80	4.38	4.65	5.84	5.69	8.39	7.03	10.9	8.79	13.7	10.2	20.3
Total inductance[+] [H]	13.3		13.3		17.0		22.3		28.4		35.1		46.9	
Stored energy @ I_{op}[+] [kJ]	419		295		340		446		513		636		756	
Bending strain [%]	0.06	0.15	0.06	0.18	0.06	0.17	0.06	0.18	0.06	0.17	0.06	0.17	0.06	0.16
Max. hoop strain [%]	0.52	0.3	0.43	0.23	0.43	0.24	0.45	0.24	0.46	0.25	0.47	0.23	0.47	0.25
Therm, hoop strain[*] [%]	−0.04	−0.05	−0.04	−0.05	−0.04	−0.05	−0.04	−0.05	−0.04	−0.05	−0.04	−0.05	−0.04	−0.05
Total hoop strain [%]	0.54	0.40	0.45	0.36	0.45	0.36	0.47	0.37	0.48	0.37	0.49	0.35	0.49	0.36
LTS magnet [MHz-mm]	1.700–237		1.700–215		1.700–228		1.600–239		1.600–254		1.500–263		1.500–285	

[*] Thermal strain by cooling from 77 K to 4.2 K

[+] only HTS insert without LTS background magnet